OCTOBER 2016

SAN FRANCISCO ESTUARY & WATERSHED SCIENCE

Sponsored by the Delta Science Program and the UC Davis John Muir Institute of the Environment

SPECIAL ISSUE: THE STATE OF BAY–DELTA SCIENCE 2016, PART 2

A Note on Delta Outflow

Stephen G. Monismith[1]

Volume 14, Issue 3 | Article 3
doi: http://dx.doi.org/10.15447/sfews.2016v14iss3art3

1 Department of Civil and Environmental Engineering
Stanford University
Stanford, CA 94305 USA
monismith@stanford.edu

ABSTRACT

Outflow from the Sacramento–San Joaquin Delta is a key parameter used in the management of the San Francisco Bay–Delta system. At present we can estimate this by assuming a steady state balance of inflows and outflows (Dayflow) or by direct measurement. In this paper, I explore differences between observed sub-tidal variations in measured outflow and Dayflow values using water level and flow data taken during the summer of 2015 and an analytical framework based on the sub-tidally filtered St. Vénant equations. This analysis shows that flows associated with sub-tidal water level variations in the Delta explain most of the difference between the two flow measures. These variations largely result from low-frequency variations in sea level in the coastal ocean and to wind stresses acting on Suisun Bay, with spring–neap variations in tides playing a lesser role. Overall, a comparison of Dayflow and the direct flow measurement for water years 2008 to 2014 shows that the two flow measures are in good agreement, although the root mean square difference between the two values (ca. 5,000 cfs) is comparable to—or larger than—typical low flow values of Dayflow.

KEY WORDS

Sacramento–San Joaquin Delta, San Francisco Bay. Suisun Bay, Suisun Marsh, Delta outflow, Dayflow, tides, salinity, wind stress, hydrodynamics

INTRODUCTION

The 2013–2015 drought, which has seen California's water supply storage brought down to historic lows, has focused attention on the management of the flow of water from the Sacramento–San Joaquin Delta (Delta) into San Francisco Bay. This "Delta Outflow" is used to maintain desired salinities in Suisun Bay and Suisun Marsh as well as to keep salinities in the Delta sufficiently low to maintain water quality for drinking and to irrigate Delta farmlands.

Current practice is to estimate Delta Outflow through the use of a hydrologic balance known as Dayflow (hereinafter denoted Q_{DF}) that is calculated by the California Department of Water Resources (CDWR c2016a). This balance includes some quantities that are measured with a relatively high degree of precision (e.g., export pumping rates), some quantities that are measured with justifiably less precision, e.g., sub-tidal (net) flows at Freeport (FPT) on the Sacramento River and Vernalis (VNS) on the San Joaquin River, and some that because they must be estimated, have a high degree of uncertainty. Notably, this latter group includes "Gross Channel Depletions" (GCD), the net flow, Q_{GCD}, from irrigation water withdrawals and returns in the Delta. Note that

Figure 1 San Francisco Bay and the Sacramento–San Joaquin Delta showing the locations of the stations used in this paper flow and water level (red circle); water level and salinity (white circle); and winds (white square box). (Image from Google Earth™)

typically in summer, as specified on a monthly basis, Q_{GCD} is ca. 3,000 to 4,000 cfs; i.e., it is comparable to—and often larger than—the stated outflow, Q_{DF}. Thus, given the uncertainty in Q_{GCD}, there can be considerable uncertainty in Q_{DF} in summer and fall.

An alternative estimate of Delta Outflow is obtained through flow data acquired at 15-minute intervals by U.S. Geological Survey (USGS) flow measuring stations in the western Delta (Oltmann 1995, 1998). These stations have been "rated" so that Acoustic Doppler Current Profiler (ADCP)-measured velocities can be used to compute flows. In this case, the instantaneous outflow is the sum of flows measured at four stations: Rio Vista on the Sacramento River (SRV), Jersey Point on the San Joaquin River (SJJ), Threemile Slough near the San Joaquin River (TSL), and Dutch Slough (DSJ) near the confluence of the two rivers, i.e.,

$$Q_{OUT} = Q_{SRV} + Q_{SJJ} + Q_{TSL} + Q_{DSJ} \quad (1)$$

Because Equation 1 includes tidal motions, to derive net outflow estimates, the measured tidally varying flows are de-tided using a Godin filter (Godin 1972).

That the two estimates do not always agree has been noted, although the degree of correspondence has never been formally addressed. Oltmann (1995) has suggested that these differences result from spring–neap filling of the Delta, although this behavior too has not been analyzed in any detail. Based on calculations of flows in the Delta using the 2D version of the circulation model TRIM3D reported in Monsen (2001), it is clear that several mechanisms may exist for creating spring–neap variations in water depths in the Delta, notably tidal stresses (the average effect of advective inertia of tidal motions) and tidal friction (the averaged effect of tidally varying bottom stresses) (c.f. Hunter 1975). I will consider these below, although the basic dynamics are that both tidal stresses and tidal friction increase the setup of the free surface required to pass flow out of the Delta. This setup requires low-frequency flows to provide the needed volume of water associated with the low-frequency changes in water level in the Delta. On the other hand, there are other means of changing sea level in the Delta; e.g., wind stresses.

The purpose of this paper is to use data to examine this flow comparison and to examine the dynamics that produce differences between measured and calculated Delta outflow. In the sections below, I will first discuss the dynamics of low-frequency variations in water surface elevation and flow heuristically. After this, I will analyze flows and

water levels measured during the summer of 2015 in light of the theoretical considerations presented earlier. In total, the summer 2015 data make clear that differences between flows measured by the USGS network and those estimated by Dayflow are not strongly associated with spring–neap tidal variations, but, rather, the strongest influences are low-frequency sea level variations in the coastal ocean and the set-up of the free surface in Suisun Bay from wind stresses.

THEORY: SUB-TIDAL MOMENTUM AND MASS BALANCES

The 2–D depth-averaged mass and momentum balances are the known as the St. Vénant equations (see, e.g., Smith and Cheng 1987 and Cheng et al. 1993). These are for conservation of mass, and x and y momentum:

$$\frac{\partial \langle \zeta \rangle}{\partial t} + \frac{\partial}{\partial x}(hU) + \frac{\partial}{\partial y}(hV) = 0 \tag{2}$$

$$\frac{\partial U}{\partial t} + g\frac{\partial \zeta}{\partial x} + U\frac{\partial U}{\partial x} + V\frac{\partial U}{\partial y} = -\frac{C_D U_b \sqrt{U_b^2 + V_b^2}}{h+\zeta} + \frac{\tau_w^x}{\rho_0 (h+\zeta)} - \frac{1}{2\rho_0}\frac{\partial \rho}{\partial x} g(h+\zeta) \tag{3A}$$

and

$$\frac{\partial V}{\partial t} + g\frac{\partial \zeta}{\partial x} + U\frac{\partial V}{\partial x} + V\frac{\partial V}{\partial y} = -\frac{C_D V_b \sqrt{U_b^2 + V_b^2}}{h+\zeta} + \frac{\tau_w^y}{\rho_0 (h+\zeta)} - \frac{1}{2\rho_0}\frac{\partial \rho}{\partial y} g(h+\zeta) \tag{3B}$$

In Equations 2 and 3 (U, V) are the instantaneous depth-averaged velocity at (x, y), ζ is the free surface elevation relative to a base depth of h, (U_b, V_b) are near-bottom velocities used to compute bottom stresses via drag coefficient C_D, (τ_w^x, τ_w^y) are surface wind stresses, ρ is the fluid density, and ρ_0 is the reference density of water (taken to be 1,000 kg m^{-3}).

To examine the dynamics of the flow with tides removed, Equations 2 and 3 are filtered with a suitable low-pass filter (e.g., the Godin filter), with the results written in terms of sub-tidal (filtered) variables and tidal variations, defined as deviations of all variables from their sub-tidal values (Walters and Gartner 1985). In this approach, any variable f is written as

$$f = \langle f \rangle + \tilde{f}$$

where

f is the instantaneous value,

$\langle f \rangle$ is the filtered value and

$\tilde{f}$ is the tidal variation, i.e., the deviation from the filtered value.

Applying this operation to Equation 2 gives

$$\frac{\partial \langle \zeta \rangle}{\partial t} + \frac{\partial}{\partial x}\left(h\langle U \rangle\right) + \frac{\partial}{\partial y}\left(h\langle V \rangle\right) = -\frac{\partial}{\partial x}\left(\tilde{\xi}\tilde{U}\right) - \frac{\partial}{\partial y}\left(\tilde{\xi}\tilde{V}\right) \tag{4}$$

http://dx.doi.org/10.15447/sfews.2016v14iss3art3

Similarly, Equation 3 becomes

$$\frac{\partial\langle U\rangle}{\partial t}+g\frac{\partial\langle\zeta\rangle}{\partial x}+\langle U\rangle\frac{\partial\langle U\rangle}{\partial x}+\langle V\rangle\frac{\partial\langle U\rangle}{\partial y}=-\left\langle\tilde{U}\frac{\partial\tilde{U}}{\partial x}\right\rangle-\left\langle\tilde{V}\frac{\partial\tilde{U}}{\partial y}\right\rangle-\left\langle\frac{C_D U_b\sqrt{U_b^2+V_b^2}}{h+\langle\zeta\rangle+\tilde{\zeta}}\right\rangle+\left\langle\frac{\tau_w^x}{\rho_o\left(h+\langle\zeta\rangle+\tilde{\zeta}\right)}\right\rangle-\frac{1}{2\rho_0}\left\langle\frac{\partial\rho}{\partial x}g\left(h+\zeta\right)\right\rangle \quad (5A)$$

and

$$\frac{\partial\langle V\rangle}{\partial t}+g\frac{\partial\langle\zeta\rangle}{\partial y}+\langle U\rangle\frac{\partial\langle V\rangle}{\partial x}+\langle V\rangle\frac{\partial\langle V\rangle}{\partial y}=-\left\langle\tilde{U}\frac{\partial\tilde{V}}{\partial x}\right\rangle-\left\langle\tilde{V}\frac{\partial\tilde{V}}{\partial y}\right\rangle-\left\langle\frac{C_D U_b\sqrt{U_b^2+V_b^2}}{h+\langle\zeta\rangle+\tilde{\zeta}}\right\rangle+\left\langle\frac{\tau_w}{\rho_o\left(h+\langle\zeta\rangle+\tilde{\zeta}\right)}\right\rangle-\frac{1}{2\rho_0}\left\langle\frac{\partial\rho}{\partial x}g\left(h+\zeta\right)\right\rangle \quad (5B)$$

These may be approximated as

$$\frac{\partial\langle V\rangle}{\partial t}+g\frac{\partial\langle\zeta\rangle}{\partial x}+\langle U\rangle\frac{\partial\langle U\rangle}{\partial x}+\langle V\rangle\frac{\partial\langle U\rangle}{\partial y}\cong-\left\langle\tilde{U}\frac{\partial\tilde{U}}{\partial x}\right\rangle-\left\langle\tilde{V}\frac{\partial\tilde{U}}{\partial y}\right\rangle-\frac{C_D\left\langle U_b\sqrt{U_b^2+V_b^2}\right\rangle}{h}+\frac{\left\langle\tau_w^x\right\rangle}{\rho_o h}-\frac{1}{2\rho_0}\frac{\partial\langle\rho\rangle}{\partial x}gh \quad (6A)$$

and

$$\frac{\partial\langle V\rangle}{\partial t}+g\frac{\partial\langle\zeta\rangle}{\partial x}+\langle U\rangle\frac{\partial\langle V\rangle}{\partial x}+\langle V\rangle\frac{\partial\langle V\rangle}{\partial y}\cong-\left\langle\tilde{U}\frac{\partial\tilde{V}}{\partial x}\right\rangle-\left\langle\tilde{V}\frac{\partial\tilde{V}}{\partial y}\right\rangle-\frac{C_D\left\langle V_b\sqrt{U_b^2+V_b^2}\right\rangle}{h}+\frac{\left\langle\tau_w^y\right\rangle}{\rho_o h}-\frac{1}{2\rho_0}\frac{\partial\langle\rho\rangle}{\partial y}gh \quad (6B)$$

It is important to note first that the filtering has produced several terms involving only tidal motions; in Equation 4 these are the wave transports (Longuet–Higgins 1969) whereas in Equation 6, these are the tidal stresses (Nihoul and Ronday 1975). Both of these can be computed from knowledge of the tides (Uncles 1982). Since the USGS measured flows are computed by filtering flows calculated from tidally-varying velocities and depths, they include wave transports as well as mean Eulerian flows.

In contrast, the filtered bottom stresses involve the combination of tidal and sub-tidal velocities. Application of Hunter's (1975) analysis of quadratic drag in the presence of energetic tides to a 1–D channel flow, shows that

$$\frac{C_D}{h}\left\langle\left(U+\tilde{U}\right)\left|U+\tilde{U}\right|\right\rangle\cong\frac{C_D}{h}\ \frac{3}{2}\langle U\rangle\left\langle\left|\tilde{U}\right|\right\rangle+\frac{\langle U\rangle}{2}\left\langle\frac{\tilde{U}^2}{\left|\tilde{U}\right|}\right\rangle \quad (7)$$

Thus, the mean bottom drag depends on both the mean flow and the tidal velocities. It is also possible that *CD* depends on flow direction (Fong et al. 2009), which would add terms to Equation 7 that involve correlations of tidally varying drag coefficients and velocities.

A bigger challenge comes from the fact that the filtered bottom stresses are based on near-bottom velocities, which may differ considerably from depth-averaged ones. Figure 2 shows an example of this: ADCP measurements made in Suisun Bay during the autumn of 2011 and early winter 2012 are shown. (See details of these measurements in the "Notes" section.) Figure 2 also shows stresses measured near-bed by the ADCP and computed using either near-bottom velocities or depth-averaged velocities are shown. Computed stresses are based on different drag coefficients for ebbs and floods. In general, measured and computed tidally varying stresses are similar to each other, and are ten times larger than sub-tidal stresses. On the other hand, the measured sub-tidal stresses are quite different from each other, even after the improvement gained by using a directionally dependent value of *CD*. Note that the near-bed baroclinic pressure gradient is also somewhat smaller than any of the sub-tidal stresses and is nearly constant, and so cannot explain the difference between the different stresses. Thus, differences between the stresses shown in Figure 2 are likely because the relationship between stresses and velocity at any fixed height involve the dynamics of the near-bed layer in a flow with time-varying stratification (Stacey et al. 1999; Stacey and Ralston 2005).

Although the dynamics of the Delta and Suisun Bay are complex and three dimensional, some insight into the low-frequency dynamics can be had through consideration of a simple model in which the Delta

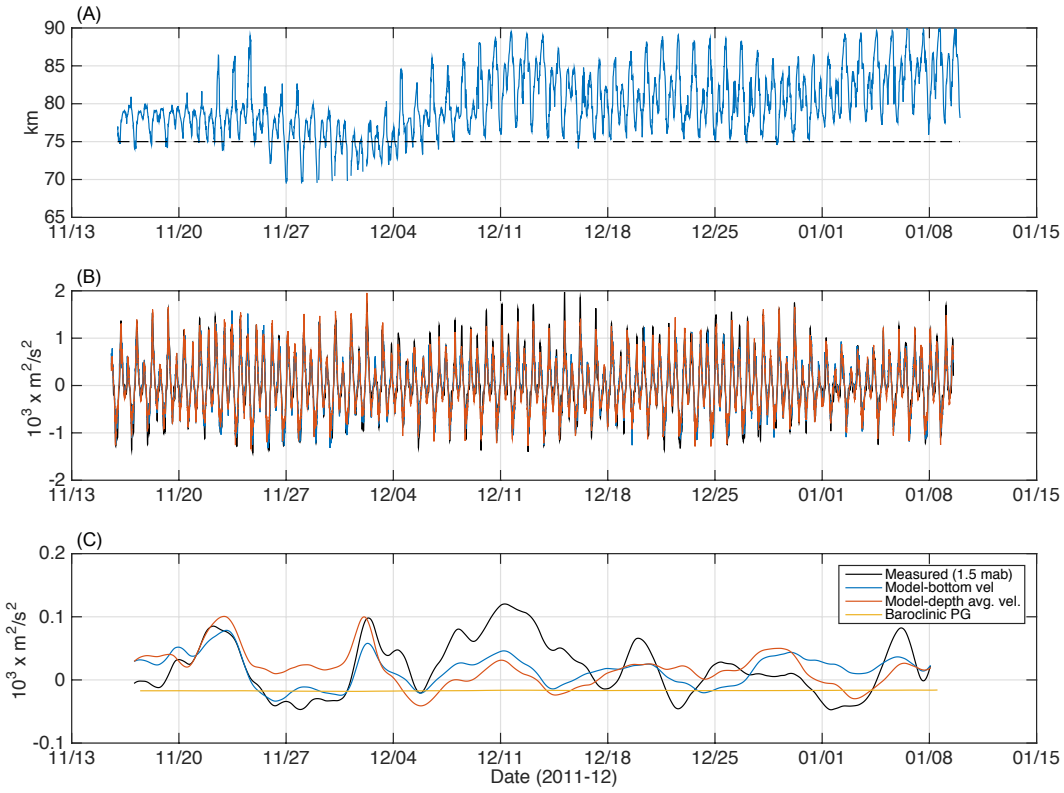

Figure 2 Data showing conditions in Suisun Bay near Chipps Island Nov 2011 to Jan 2012: (A) instantaneous X2 – the dashed line shows the position of the ADCP used to measure flows and stresses; (B) stresses measured at 1.5 mab (black line), computed using a quadratic drag law and the velocity at 1.5 mab (blue line) with a directionally dependent value of CD, and computed using a quadratic drag law and depth-averaged velocities and a directionally dependent value of CD (red line); (C) Godin-filtered stresses as in (B) plus baroclinic pressure gradient (yellow line)

is essentially a reservoir in which the sub-tidal water level variations are nearly constant across the Delta and Suisun Bay is a 1–D channel that extends from Martinez in the west to Mallard Slough (Chipps Island) in the east (Figure 3). Some evidence for this model based on 2–D and 3–D flow computations is presented in Monsen (2001). In the present simple model, the sub-tidal dynamics embodied in Equations 6 and 7 (albeit recognizing the potential errors in the bottom stress representation) are assumed to be 1–D and quasi steady. Thus, the sub-tidal momentum balance of Suisun Bay determines the change in water level between Martinez and Mallard Slough, whereas the water level in the Delta is approximately the same as that at Mallard Slough.

If the continuity equation is integrated over the Delta, then:

$$A_D \frac{\partial \overline{\langle \zeta \rangle}}{\partial t} = Q_{SAC} + Q_{SJR} + Q_{MI} - Q_{EXP} - Q_{MD} - Q_{OUT} \quad (8)$$

where $\overline{\langle \zeta \rangle}$ is the average height of the free surface in the Delta, $A_D \approx 3 \times 108\,\mathrm{m}^2$ is the surface area of the Delta, Q_{SAC} and Q_{SJR} are the river inflows, Q_{MI} represents the other inflows included in Dayflow, Q_{EXP} is the export pumping, Q_{GCD} are the unmeasured in-Delta diversions, Q_{MD} represents the other, smaller diversions in the Delta, and Q_{OUT} is the outflow from the Delta. Note that Q_{OUT} includes both mean flows and wave transports, since the filtered value of the instantaneous measurement of the flow out includes both components. Also note that all of the terms on the right-hand side (rhs) of Equation 8 are included in Dayflow with Q_{OUT} computed by assuming that the left-hand side (lfs) of Equation 8 is zero. Thus, according to Equation 8, allowing for storage in the Delta implies that

http://dx.doi.org/10.15447/sfews.2016v14iss3art3

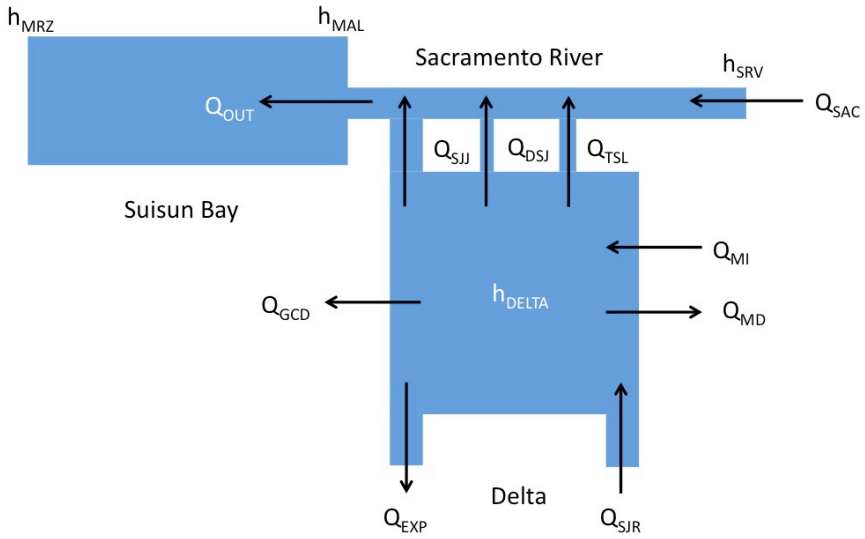

Figure 3 Schematic of an idealized Delta and Suisun Bay for model. Note that the connection of the Sacramento River via the Delta Cross Channel and Georgiana Slough is not shown.

$$Q_{OUT} = Q_{DF} - A_D \frac{\partial \overline{\langle \zeta \rangle}}{\partial t} = Q_{DF} - Q_{FE} \tag{9}$$

where, as defined by Equation 9,

$$Q_{FE} = A_D \frac{\partial \overline{\langle \zeta \rangle}}{\partial t}$$

is the flow associated with the filling and emptying of the Delta. Thus, assuming that both Dayflow and the USGS flow measurements are accurate, we should expect that measured flows out of the Delta should differ from Dayflow values by an amount that depends on the filling and emptying of the Delta (Oltmann 1998).

Assuming steady state, that cross-sectional (y) variations are small, and that the wind stress and depth are constant, the along-channel sub-tidal momentum balance (Equation 6A) can be integrated from $x = 0$ at Martinez and $x = L$ at Mallard Slough to find that

$$\langle \zeta \rangle \Big|_0^L \cong -\frac{1}{2g} \langle \tilde{U}^2 \rangle \Big|_0^L - \frac{C_D}{gh} \int_0^L \frac{3}{2} \langle U \rangle \langle |\tilde{U}| \rangle + \frac{\langle U \rangle}{2} \left\langle \frac{\tilde{U}^2}{|\tilde{U}|} \right\rangle dx + \frac{\langle \tau_w^x \rangle L}{\rho_0 g h} - \frac{h}{2\rho_0} \langle \rho \rangle \Big|_0^L \tag{10}$$

Thus, the set-up of the water surface—and hence, the filling and emptying of the Delta—depends on changes in tidal velocities across Suisun Bay, mean and tidal flows in Suisun Bay, wind stresses on the Suisun Bay, and the density difference across Suisun Bay.

METHODS: DATA AND PROCESSING

I extracted all data used in what follows from online sources: the California Data Exchange Center (CDEC c2012) and the National Oceanic and Atmospheric Administration's (NOAA) PORTS™ San Franciso Bay archives (NOAA c2013). These sources contain data collected by the California Department of Water Resources (CDWR), the U.S. Bureau of Reclamation, the USGS and NOAA. In all cases, data downloaded described the period from June 1, 2015 to September 30, 2015, a period of relatively low flow that should be ideal for evaluating the effects of the filling and emptying of the Delta on outflow.

Water level data was obtained for the Golden Gate (NOAA Station 9414290), Martinez (MRZ), Mallard Slough (MAL), the Sacramento River at Rio Vista (SRV), the San Joaquin River at Jersey Point (SJJ), the Old and Middle rivers (OH), and the San Joaquin River at Mossdale (MSD). Salinity data was also obtained for Martinez and Mallard Slough. I chose these stations as representative of Suisun Bay (MRZ and MAL), and the Sacramento (SRV) and San Joaquin (SJJ, OH, and MSD) sides of the Delta. I obtained flow data for the four USGS flow stations (SRV, TSL, DJJ, and SJJ) that serve to define flows exiting the Delta, as well as for flows down the Old and Middle River corridor (OMR). Dayflow data for water year (WY) 2015 was also downloaded from the CDWR website (CDWR c2016b). I obtained wind speed and direction data for Suisun Bay from SFPORTS for the NOAA weather station located on Suisun By near Pittsburgh (Station 9415115).

To examine sub-tidal behavior of flows and water level, the instantaneous (generally 15-minute) data (water levels and flow) was low-pass filtered using a Godin filter. Short gaps (< 1 hr) were filled via linear interpolation. I converted wind speed data to wind stresses by using a quadratic drag law with a drag coefficient of 1.3×10^{-3} (c.f. Fischer et al 1979). In what follows, I used only the east–west component of the wind stress vector to calculate set-up on Suisun Bay.

Since the exact elevation of each pressure sensor is not known, to facilitate comparison of time-varying water levels from the various stations, I subtracted the mean depth from each signal. In terms of assessing the mechanisms for the filling and emptying of the Delta, this has no effect on the results of the analysis, since only temporal changes in water level produce flows (c.f., Equation 9). However, this does mean that it is also necessary to subtract the mean value of forcing terms—e.g., the wind stress—when analyzing the effects of winds on Bay–Delta water levels. In what follows, negative changes in any variable means that the given variable is less than its average value. In particular, since prevailing winds are west to east, Suisun Bay should generally set up with higher water levels in the east. In the analysis presented here this will mean that although wind stresses weaker than the average wind stress will produce apparently negative values of computed set-up, the actual set-up would still be positive if the unknown mean value were added to the computed value.

RESULTS

Water level and flow data for the Bay–Delta region for the summer of 2015 are shown in Figure 4. Several features of the way water levels vary in the Delta stand out. Firstly, as expected, tidal heights decrease from the Golden Gate to the rivers (Figure 4B). Secondly, sub-tidal depth variations in the Delta stations are nearly constant, and do not appear to have any particular relation to variations in root mean square (rms) tidal heights, i.e., to the spring–neap cycle. Delta water levels also follow water level variations in Suisun Bay and at the Golden Gate. These connections are examined more formally in the "Discussion."

Net flows out of the Delta as determined by the USGS flow network (Q_{USGS}) are substantially larger in magnitude and often of different sign than are Dayflow calculated values and export pumping (Figure 4D). On the other hand, variations in Q_{USGS} closely follow variations in Q_{OUT}. This variation can be examined more closely by looking at the dependence of the difference between *QUSGS* and *QDF* as a function of *QFE*. As seen in Figure 5, the difference between measured and calculated outflows is tightly correlated ($r^2 = 0.987$ as determined by robust fitting) with flows associated with changes in water volume in the Delta, i.e.:

$$Q_{USGS} - Q_{DF} = (0.65 \pm 0.05) Q_{FE} + (13 \pm 260) \qquad (11)$$

http://dx.doi.org/10.15447/sfews.2016v14iss3art3

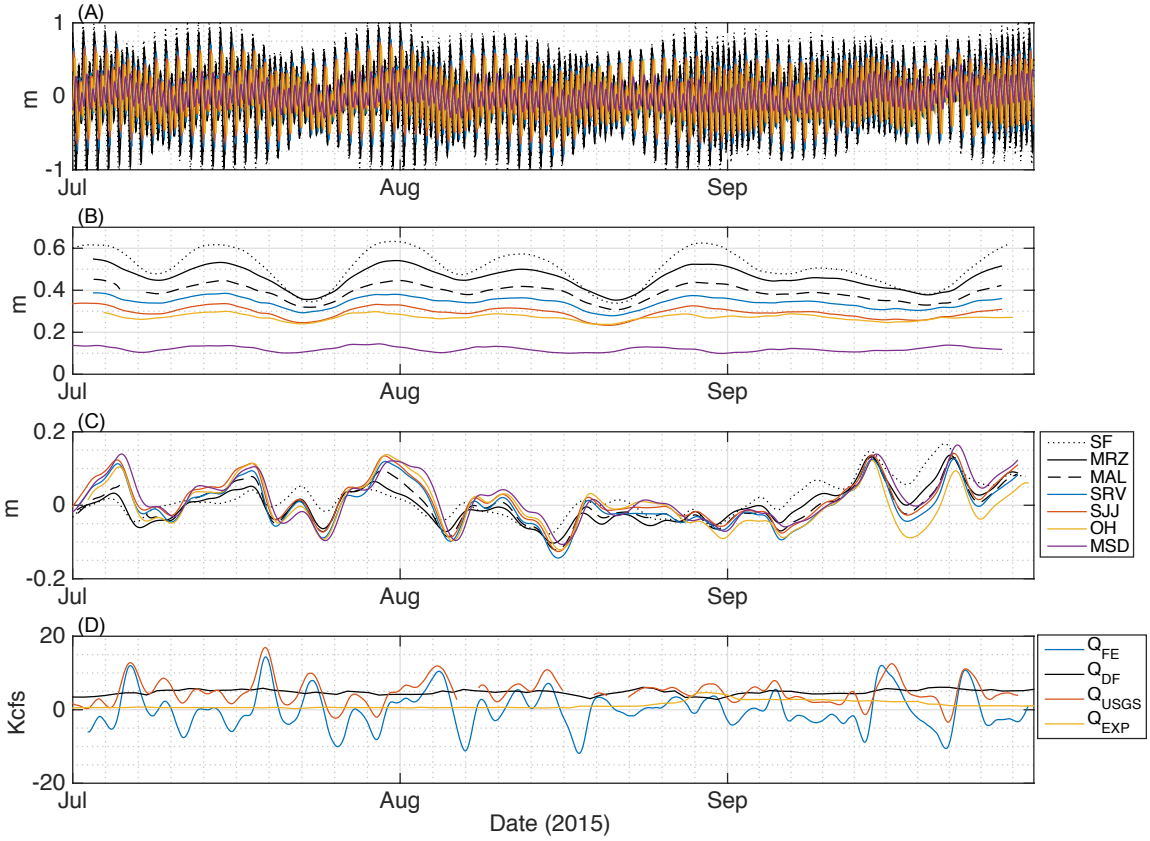

Figure 4 Water levels and flows in the San Francisco Bay and Sacramento–San Joaquin Delta in the summer of 2015: **(A)** total water level variations; **(B)** RMS tidal variations in water levels; **(C)** sub-tidal variations in water levels; and **(D)** sub-tidal flows. The legend in panel **(C)** applies to panels **(A)** through **(C),** whereas the legend in panel **(D)** applies only to that panel.

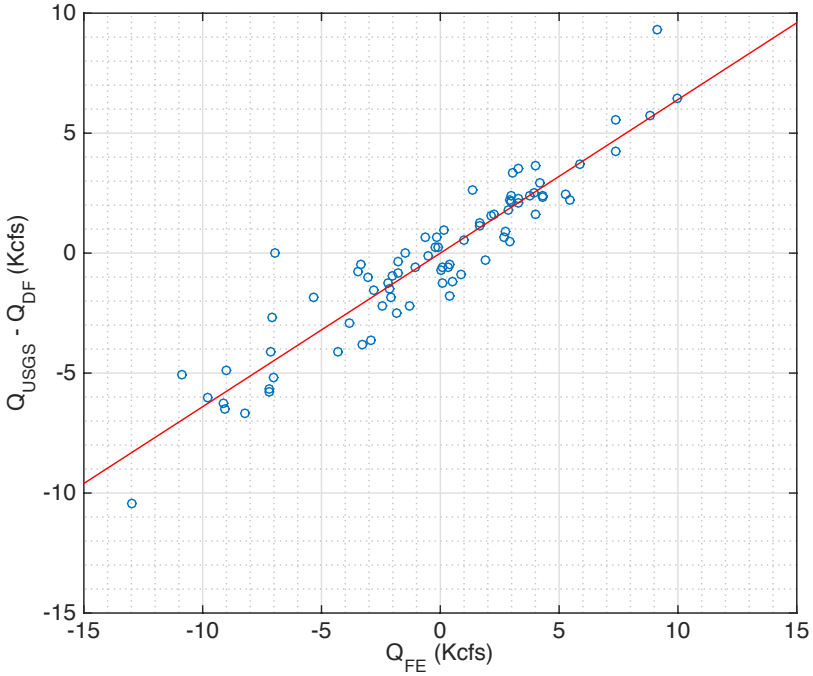

Figure 5 The difference between USGS measured flows (Q_{USGS}) and calculated Dayflow values (Q_{DF}) as a function of the flow associated with filling and emptying the Delta (Q_{FE}). The linear fit shown (red line) is $Q_{USGS} - Q_{DF} = (0.65 \pm 0.05)\ QFE + (13 \pm 260)$ (all values in cfs) has $r^2 = 0.88$ as determined by least-squares fitting

with an root-mean-square (rms) error of of 1,160 cfs. Equation 11 suggests that the effective value of AD for filling and emptying is $2 \times 10^8\,m^2$ not $3 \times 10^8\,m^2$. This likely reflects the fact that although tightly co-varying, sub-tidal water level changes in the Delta are not entirely uniform. Thus, the simple estimate of the filling–emptying flow presented above could be improved by using Equation 9 with all of the available water level records in the Delta. Most importantly, as Oltmann (1995, 1998) suggested, and to a remarkable extent, the differences between flows measured by the USGS flow network and those calculated by Dayflow (at least for summer 2015) can clearly be attributed to the filling and emptying of the Delta.

Given that the filling and emptying of the Delta during dry periods produces large variations in outflow, it is important to understand the sources of that variability. Given the discussion in "Theory: Sub-Tidal Momentum and Mass Balances" and that Delta water levels seem strongly correlated with water levels at Martinez, a simple empirical model for water level in the Delta would be

$$H_{Delta} = AH_{SF} + B\left(\xi_{ms} - \overline{\xi_{ms}}\right) + C\frac{\left\langle \tau_w^x \right\rangle L}{\rho h} \qquad (12)$$

where

$$H_{Delta} = \left\langle \xi_{Delta} \right\rangle - \left\langle \overline{\xi_{ms}} \right\rangle$$
$$H_{SF} = \left\langle \xi_{SF} \right\rangle - \overline{\left\langle \xi_{SF} \right\rangle} \qquad (13)$$
$$\xi_{ms} = \left\langle \left(\tilde{\xi}_{MRZ} \right)^2 \right\rangle^{1/2}$$

and $\overline{f}$ is the average of a variable f over the entire record. The reason for a possible linear dependence on rms tidal variation is the fact that the integral term in Equation 10 is proportional to the product of Q_{OUT} and the tidal velocity, and so should vary through the spring–neap cycle. Equation 12 does not include any dependence on the square of the rms tidal height variation, a dependence suggested by Equation 10. This is because that first term on the rhs of Equation 10 should vary with the square of the tidal velocity and, thus (more approximately), with the square of the variation in tidal height, but can be computed from measurements (or computations) of tidal velocities at the two ends of Suisun Bay. The rms velocity in Carquinez Strait near Martinez can be estimated to be 0.66 m s^{-1} from the measurements shown in Stacey et al. (2001), whereas at Mallard slough, the rms velocity is 0.56 m s^{-1}. (See details of these measurements in the "Notes" section.) Thus, the set-up associated with the change in tidal velocity should be 0 (6 mm), i.e., quite small.

Equation 12 was fit to the observations using the functions *ftlim* and *anova* from the Matlab™ statistics toolbox. This fit shows that San Francisco water level, spring–neap tide modulations and wind stress are all important determinants of water level variations, explaining 29%, 14%, and 39% of the variance, respectively (Table 1; Figure 6). Given that the p values for the fitting of each of these variables are essentially 0, these are robust results. Thus, although the spring–neap tidal cycle plays a lesser role than either coastal ocean sea level variations or wind stresses on Delta water levels, it is not insignificant. Cross-spectral analysis of the San Francisco water level data (not presented here) shows that low-frequency

Table 1 Parameters in Equation 12

	Parameter	Value	Variance %
SF height	A	0.80 ± 0.05	29
Tide rms	B	0.52 ± 0.04	14
Wind stress	C	1.07 ± 0.05	39

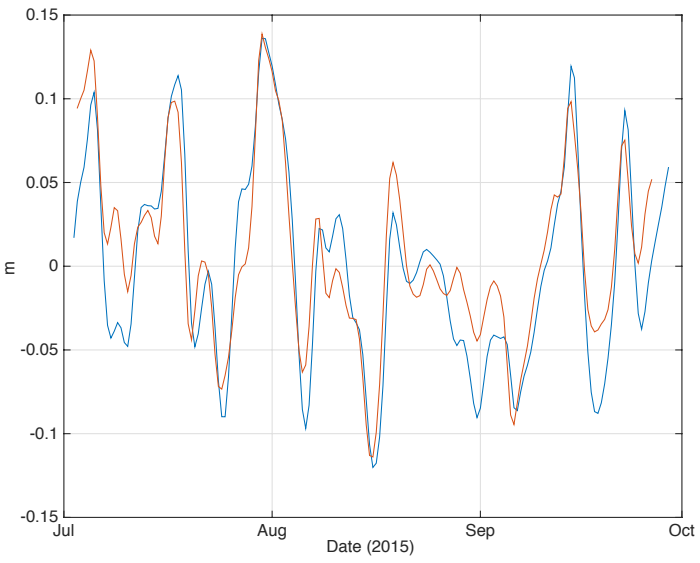

Figure 6 Sub-tidal height variations in the Delta: observed (blue line); linear fit with SF height variations, wind stress, and rms tidal height variations (red line) using Equation 12

http://dx.doi.org/10.15447/sfews.2016v14iss3art3

San Francisco water levels are essentially independent of rms tidal height variations, so including H_{SF} as an explanatory variable does not mask the apparent importance of spring–neap tidal variations.

The dynamical significance of the winds can be seen directly in the integrated form of the sub-tidal momentum given in Equation 10. If wind stress only is included:

$$\langle \zeta \rangle \Big|_0^L \cong \frac{\langle \tau_w^x \rangle L}{\rho_0 h} \tag{14}$$

Using Equation 14, the set-up for Suisun Bay (L = 20 km) is moderately well predicted (r^2 = 0.76) if the Pittsburg wind stress is multiplied by a factor of 0.39 (Figure 7).

The baroclinic pressure gradient term, something not included in Equation 12, can be calculated from measured salinities, or from knowledge of X2 using the approximation to the mean salinity gradient given by Monismith et al. (2002) as:

$$\frac{h}{2\rho} \langle \rho \rangle \Big|_0^L \simeq 2.6 \times 10^{-5} \frac{h}{2} \frac{L}{X2} \tag{15}$$

Examination of the dependence of X2 on spring–neap tidal variations for the period 1999–2012 (analysis not shown), indicates that only ca. 1% of the variance in X2 is associated with spring–neap tidal variations. Thus, the baroclinic pressure gradient term is likely to only have a weak dependence on the spring–neap cycle. On the other hand, it can represent a measurable steady set-up of the free surface: e.g. given h = 12 m, $\rho_0 \simeq$ 1000 kg m^{-3}, and L = 20 km, for X2 = 80 km, Equation 15 gives a set-up of 0.035 m. Throughout the summer period of interest, the calculated set-up from baroclinic effects varied by ca. ± 5 mm, producing effective flows of 0 (±100 cfs) per Equation 9 (Figure 8), i.e., values that are somewhat smaller than what is seen in Figure 4 (see also Walters and Gartner 1985).

It does appear that the low frequency sea level changes discussed above affect salinity in a way that is consistent with the flows they produce (Figure 9). When sea level rises, Delta outflow is reduced (or even becomes negative), X2 moves upstream, and salinity increases. For bottom salinities and heights at Mallard Slough, the linear scaling that predicts salinity variations from height variations:

$$\langle S_{MAL} \rangle - \overline{\langle S_{MAL} \rangle} = 12 \left\{ \langle \zeta_{MAL} \rangle - \overline{\langle \zeta_{MAL} \rangle} \right\} \tag{16}$$

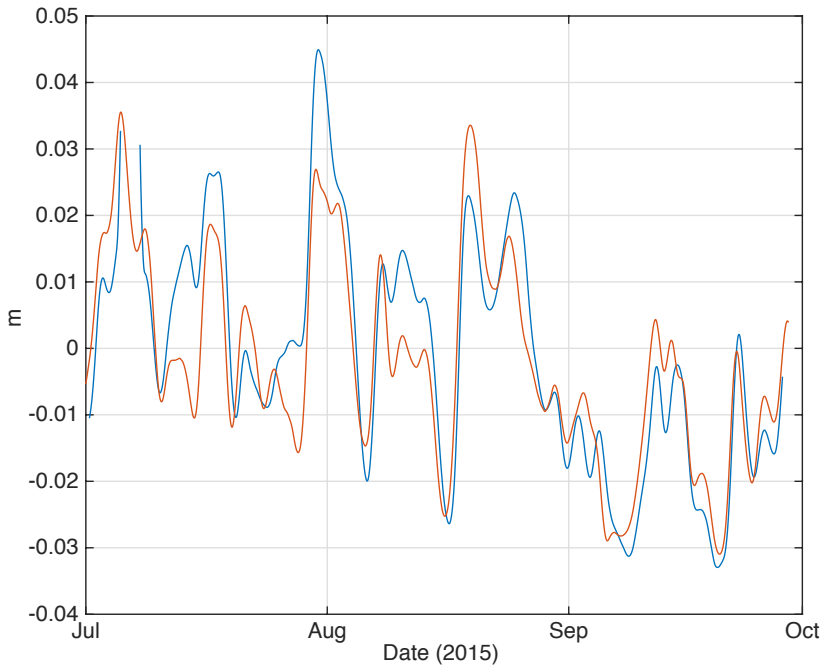

Figure 7 Variation of the set-up of the water surface in Suisun Bay: observed (blue line) and from wind stress (red line) value calculated using Equation 14 and multiplied by 0.39

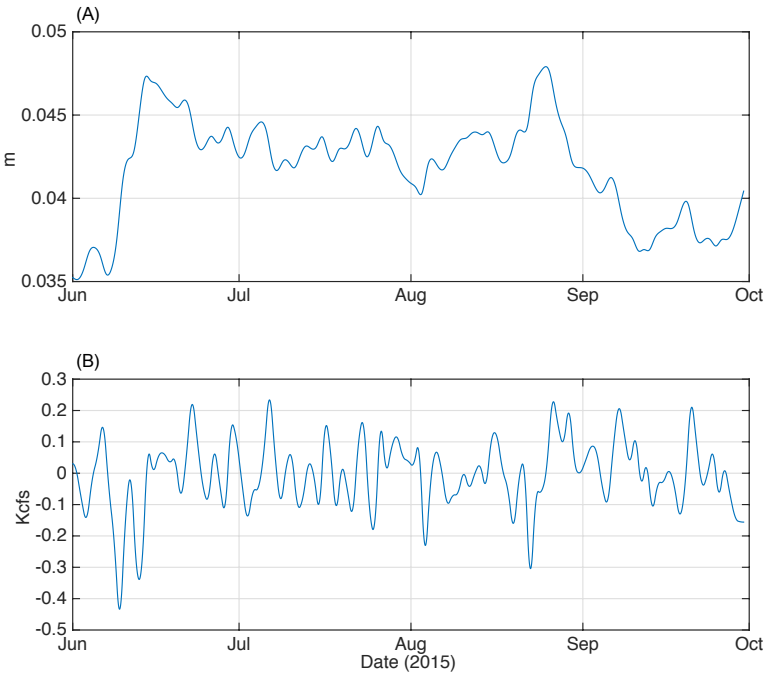

Figure 8 **(A)** Set-up of Suisun Bay as a result of baroclinic pressure gradients calculated using Equation 15 and using salinities measured at MAL and MRZ; **(B)** flows associated with changes in baroclinic set-up estimated using Equation 9

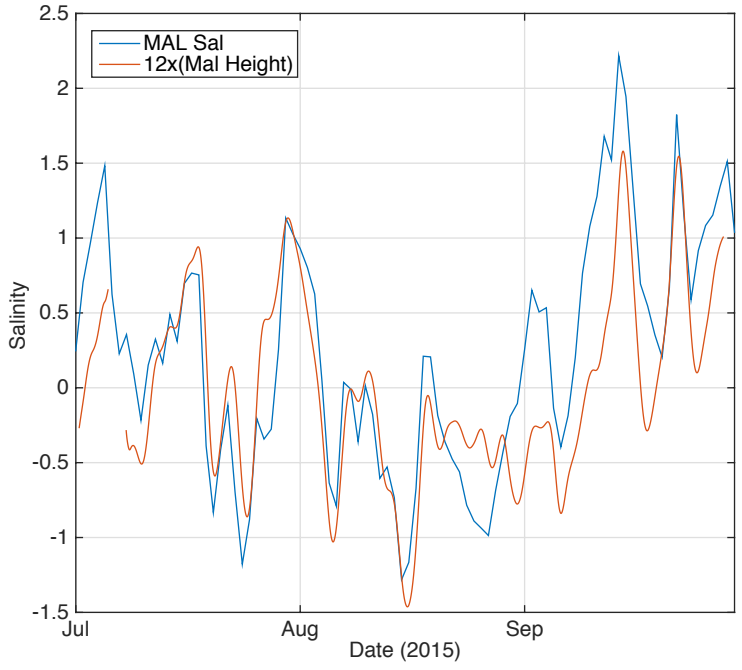

Figure 9 Salinity variations relative to record mean values at Mallard Slough measured (blue) and predicted from water level at Mallard Slough (red)

explains 55% of the variance in salinity. Despite presumed connections between salinity intrusion and the spring–neap tidal cycle (MacCready 1999), rms tidal height variations have almost no discernible effect on salinity, i.e., rms height variations explain none of the salinity variance. This may be because X2 during this period was reasonably large (90 to 100 km) and so salt fluxes from gravitational circulation would likely have been weak. Thus, the increase in upstream transport of salt by gravitational circulation that would occur at neaps may have been offset by the simultaneous decrease in salt transport by tidal mixing (Fischer et al 1979), so that little effect of the spring–neap cycle would be seen in measured salinities.

DISCUSSION AND CONCLUSIONS

The analysis presented above makes clear three points: (1) that filling and emptying of the Delta explains a significant component of the O (± 10 Kcfs) differences between USGS measured sub-tidal outflows from the Delta and values computed by the CDWR using the Dayflow methodology for summer 2015; (2) that filling and emptying of the Delta during this time was associated with low frequency variations of sea level in the coastal ocean that are also seen in Suisun Bay, with wind stresses acting on Suisun Bay; and (3) that, as suggested by Oltman (1995) and others, spring–neap modulations in tidal heights, although this latter effect appears to have less influence than do the first two factors.

The result that coastal ocean sea level variability and local wind stresses are major contributors to sea level variability in the Bay–Delta is not new: Walters and Gartner (1985) found that at sub-tidal frequencies, northern San Francisco Bay responded coherently to coastal sea level changes. For South San Francisco Bay, Walters (1982) found that set-up in response to local winds on the Bay also affected low-frequency sea level variability. In the present case, for low flows, the same appears to be true for Suisun Bay and the Delta, a relation that may break down when Delta inflows and outflows are large.

http://dx.doi.org/10.15447/sfews.2016v14iss3art3

The analyses of Walters and Gartner (1985) and later Ryan and Noble (2007) were based on the use of Empirical Orthogonal Functions (EOFs—e.g., see Emery and Thomson 2001). EOF analysis is a way to examine the spatial and temporal structure of correlations of a set of data, in this case, a time-series of water surface elevation. In this approach, a vector of time-series h_i measured at $x=x_i$ is constructed as

$$h_i = \sum_{j=1}^{N} A_j(t)\phi_j(x_i) \qquad (17)$$

where the A_j is the time-series of the j^{th} empirical mode (EOF), which has spatial variation $\phi_j(x)$. For N time-series, there are N EOFs. Computed as the eigenvectors of the covariance matrix of the h_i, the EOFs are chosen so that the first mode explains the maximum amount of variance in the original set of time series, the second mode explains the next largest amount, and so forth.

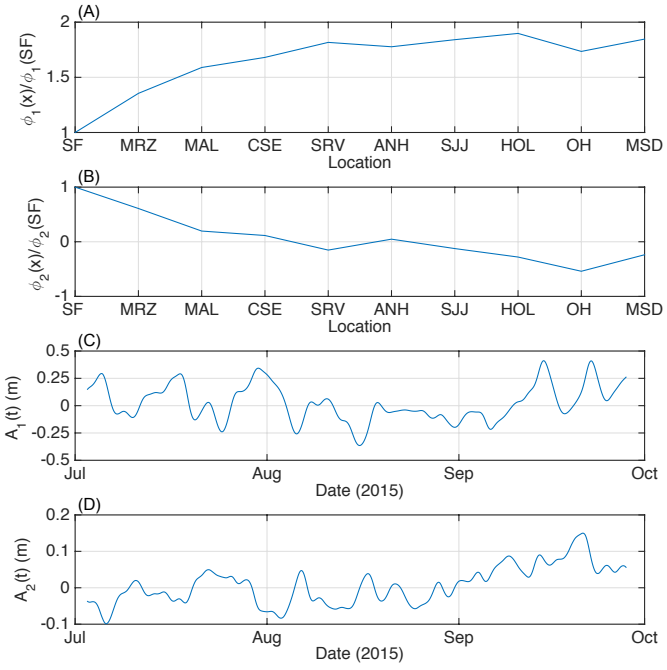

Figure 10 Results of EOF analysis of northern San Francisco Bay and Delta water levels: **(A)** spatial variation in amplitude of mode 1; **(B)** spatial variation in amplitude of mode 2; **(C)** temporal variation in amplitude of mode 1; and **(D)** temporal variation in amplitude of mode 2. The labels in panels **(A)** and **(B)** refer to CDEC stations, except for SF, which refers to the NOAA station at Fort Point. Note that $\phi_1(SF) = 0.19$ and $\phi_2(SF) = 0.73$.

Results of this analysis (now including additional CDEC water level stations processed earlier) are shown in Figure 10 for summer 2015 where the first mode, which explains nearly 90% of the overall variance in the data, can be seen to demonstrate a strong covariance of all stations (Figure 11A). The ratio of the value of ϕ_1 at MRZ to that at SF is quite close to what Walters and Gartner describe: 1.35 vs. 1.32. In a similar fashion, they found this ratio at Port Chicago to be 1.53 vs. the present value of 1.59 at Mallard Slough, 10 km east of Port Chicago. Similarly, the second mode, which explains 9% of the variance, follows the behavior seen by Walters and Gartner, i.e., stations in the west vary in opposite fashion to those in the east.

The behavior of the second mode is easily described, since approximately 50% of its variance is explained using the Pittsburgh wind stress: it represents the set-up of northern San Francisco Bay by the prevailing winds. On the other hand, the first mode is more

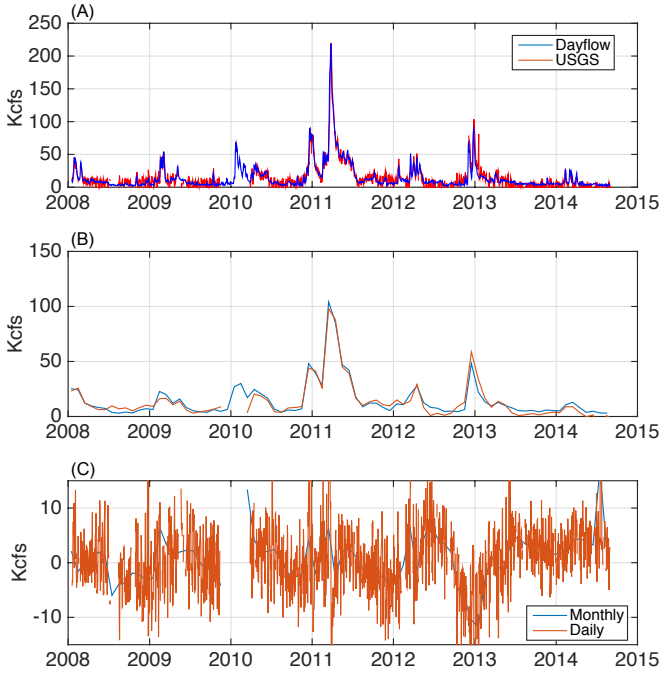

Figure 11 Comparison of USGS and Dayflow derived outflows: **(A)** plots of Dayflow (blue line) and Godin-filtered USGS outflow (red line); **(B)** Monthly averages of the flows plotted in **(A)**; **(C)** differences between Dayflow and USGS outflows for monthly (blue line) and daily (red line) values

challenging to explain, in that it is not significantly correlated with either the wind stresses or with the spring–neap tidal cycle. As suggested by Walters and Garther (1985) and Ryan and Noble (2007), it may represent water level variations forced by coastal sea level variations. On the other hand, it is difficult to imagine how very low-frequency sea level variations might be amplified by almost a factor of 2 as they propagate into the Delta, since what might be expected would be a pure co-oscillation of the Suisun Bay and Delta with offshore, possibly with a reduction due to frictional damping. Indeed the analysis presented above (c.f. Table 1), including San Francisco Bay water levels as an independent variable does suggest a damping of coastal water level variations in the Delta. Moreover, the first analysis suggests a much larger effect of winds than does the EOF analysis (40% vs. 5% of Delta water level variability). Given that the Analysis of Variance (ANOVA) gives physically reasonable results and the EOF analysis results are difficult to explain—at least for the first mode—it would seem that the ANOVA results offer a better description of what drives low-frequency variability in the Delta. Finally, given that values of ϕ_1 for all the eight Delta stations (MAL to MSD) are within 10% of the average value for this set of stations, the assumption used to derive Equation 8—that the low-frequency variability of the water surface in the Delta is nearly uniform—seems reasonable.

To put these results in context, examining the overall comparison of USGS flows and Dayflow is worthwhile. Figure 11 shows a plot of the comparison of the two flows for water years 2008–2014. Overall, for the full range of flows, the comparison is excellent, particularly after averaging the two flows over months (Figure 11B), although the difference between the two flow measures seems to be significant over seasonal time-scales starting in 2012. As one reviewer of this paper suggested, this may result from the fact that GCD may not accurately represent actual channel depletions during a drought. Linear fitting of the entire data set (Figure 12A) gives

$$Q_{USGS} = 1.02 Q_{DF} - 703\,, \tag{18}$$

with $r^2 = 0.94$ and an rms error of 5,500 cfs. However, fitting only to Dayflow values less than 10 Kcfs (Figure 12B), gives

$$Q_{USGS} = 0.88 Q_{DF} - 24\,, \tag{19}$$

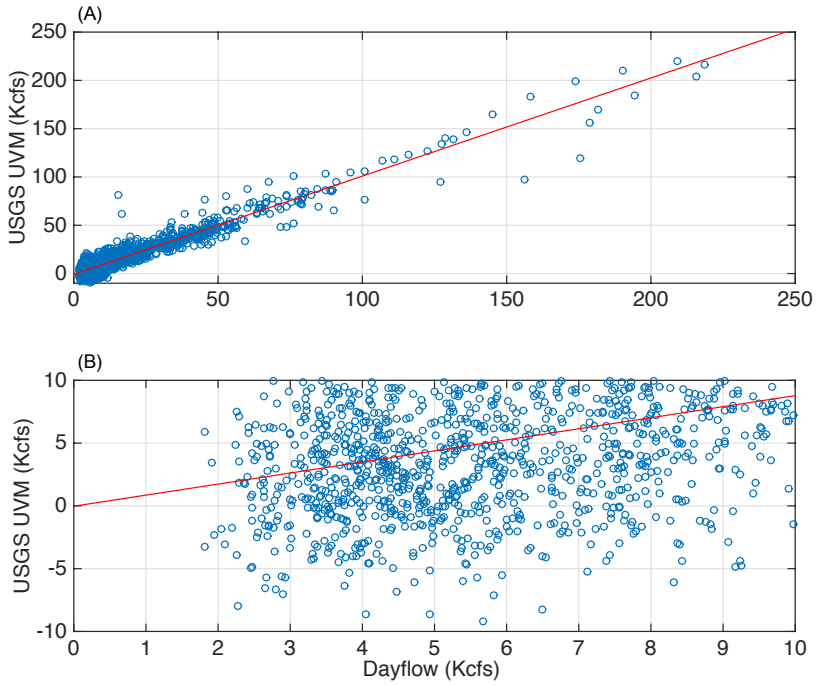

Figure 12 Comparisons of Dayflow and USGS outflow: **(A)** the full range of flows for WYs 2008–2014; **(B)** for flows < 10 Kcfs. In both cases, the red line is the least square fit to the data.

http://dx.doi.org/10.15447/sfews.2016v14iss3art3

although this fit has almost no significance (r^2 = 0.05) and has a standard error (5,310 cfs) comparable to that of the full data set.

Thus, over the longer record of measured flows, it would appear that Dayflow over-estimated by 610 ± 140 cfs the outflows measured by the USGS flow network. The reasons for this difference are not clear, although it may be the case that Dayflow under-estimated in-Delta diversions. On the other hand, the fact that the sub-tidal flows at Rio Vista are only a few percent of the tidally varying flow suggests that direct measurement of Delta outflow during dry periods, when it is relatively small, may not be possible using normal gauging procedures.

For the present, given the uncertainty in Dayflow associated with uncertainty in in-Delta diversions, it would appear that when Dayflow is small, the error in estimated outflow is likely as large as—or larger than—Dayflow itself. As shown above, in addition to this error there are large calculable variations in flow from the filling and emptying of the Delta associated with spring–neap tidal variations, winds on Suisun Bay, and ultimately from water level changes in the coastal ocean.

Finally, it seems that the analysis presented above (see also Monsen 2001), might be usefully pursued in more depth using 3–D numerical modeling to examine the sub-tidal momentum balance, e.g., to explicitly include the tidally varying bottom friction, although to do so would require careful consideration of the likely accuracy of the calculations, since small errors at tidal time-scales might accumulate into large errors at sub-tidal time-scales.

Unfortunately, given that the actual flow is unknown, it is difficult at present to say which of the two estimates is more accurate. Thus, given the management need of accurately connecting reservoir releases to regulation-mandated outflows during dry periods, it would seem important to improve Delta outflow estimation. At present, the best alternative appears to be to do as MacWilliams et al. (2015) suggested; use variations in salinity predicted by accurate 3–D models to infer flows. An alternative approach would be to directly measure net diversions in the Delta, something that would require both measurements of diversions and returns, as well as estimation of exchanges with Delta channels through groundwater flows. Although this is likely to be politically difficult to implement, it might enable direct quantification of low-flow outflows.

ACKNOWLEDGEMENTS

This work was partially supported by the United States Bureau of Reclamation through agreement R12AC20005 and by the Delta Stewardship Council Science Program. The author gratefully acknowledges the thoughtful reviews provided by two anonymous reviewers.

REFERENCES

[CDEC] California Department of Water Resources. c2012. California Data Exchange Center [Internet]. [Accessed from 05 Dec 2015 to 05 Jan 2016]. Available from: *http://cdec.water.ca.gov*

[CDWR] California Department of Water Resources. c2016a. Dayflow documentation [Internet]. [Accessed 05 Dec 2015]. Available from: *http://www.water.ca.gov/dayflow/documentation/dayflowDoc.cfm#Introduction*

[CDWR] California Department of Water Resources. c2016b. Dayflow database. [Internet]. [Accessed 14 Dec 2015]. Available from: *http://www.water.ca.gov/dayflow/output/Output.cfm*

Cheng RT, Casulli V, Gartner JW. 1993. Tidal, residual, intertidal mudflat (TRIM) model and its applications to San Francisco Bay, California. Estuarine Coast Shelf Sci 49:647–665. doi: *http://dx.doi.org/10.1006ecss.1993.1016*

Emery WJ, Thomson RE. 2001. Data analysis methods in physical oceanography. Amsterdam (Netherlands): Elsevier Press. 716 p.

Fischer HB, List EJ, Imberger J, Koh RCY, Brooks NH. 1979. Mixing in inland and coastal waters. New York (NY): Academic Press. 302 p.

Fong DA, Monismith SG, Burau JR, Stacey MT. 2009. Observations of secondary circulation and bottom stress in a channel with significant curvatures. J ASCE Hyd Div 135(3):198–208. doi: *http://dx.doi.org/10.1061(ASCE)0733-9429(2009)135:3(198)*

Godin G. 1972. The analysis of tides. Toronto (BC): University of Toronto Press. 264 p.

Hunter JR. 1975. A note on quadratic friction in the presence of tides. Estuarine Coast Mar Sci 3:473–475. doi: *http://dx.doi.org/10.1016/0302-3524(75)90047-X*

Longuet–Higgins, M. 1969. On the transport of mass by time-varying ocean currents. Deep–Sea Res 16:431–447. doi: *http://dx.doi.org/10.1016/0011-7471(69)90031-X*

MacCready P. 1999. Estuarine adjustment to changes in river flow and tidal mixing. J Phys Oceanogr 29:708–726. doi: *http://dx.doi.org/10.1175/1520-0485(1999)029<0708:EATCIR>2.0.CO;2*

MacWilliams ML, Bever AJ, Gross ES, Ketefian GS, Kimmerer WJ. 2015. Three-dimensional modeling of hydrodynamics and salinity in the San Francisco Estuary: an evaluation of model accuracy, X2, and the low-salinity zone. San Franc Estuary Watershed Sci 13(1). doi: *http://dx.doi.org/10.15447/sfews.2015v13iss1art2*

Monismith SG, Kimmerer W, Stacey MT, Burau JR. 2002. Structure and flow-induced variability of the subtidal salinity field in Northern San Francisco Bay. J Phys Oceanogr 32(11):3003–3019. doi: *http://dx.doi.org/10.1175/1520-0485(2002)032<3003:SAFIVO>2.0.CO;2*

Monsen NE. 2001. A study of subtidal transport in Suisun Bay and the Sacramento–San Joaquin Delta, California [dissertation]. [Stanford CA]: Stanford University.

Nihoul JC, Ronday FC. 1975. The influence of tidal stress on the residual circulation. Tellus 21:484–489. doi: *http://dx.doi.org/10.1111/j.2153-3490.1975.tb01701.x*

[NOAA] National Oceanic and Atmospheric Administration. c2013. San Francisco Bay PORTS™ [Internet]. [Accessed 13 Dec 2015] [Updated 15 Oct 2013]. Available from: *http://tidesandcurrents.noaa.gov/ports/index.shtml?port=sf*

Oltmann RN. 1995. Continuous flow measurements using ultrasonic velocity meters: an update. [Internet]. [Accessed 15 Oct 2015]. Interagency Ecological Program for the San Francisco Estuary Newsletter 8(4):22–25. Available from: *http://www.water.ca.gov/iep/newsletters/1995/fall/page22.pdf*

Oltmann RN. 1998. Indirect measurement of Delta outflow using ultrasonic velocity meters and comparison with mass balance calculated outflow. [Internet]. [Accessed 27 Dec 2015]. Interagency Ecological Program for the San Francisco Estuary Newsletter 11:5–8. Available from: *http://www.water.ca.gov/iep/newsletters/1998/winter/Indirect%20Measurement%20of%20Delta%20Outflow%20Using%20Ultrasonic%20Velocity%20Meters.pdf*

Ryan HF, Noble M. 2007. Sea level fluctuations in central California at subtidal to decadal and longer time scales with implications for San Francisco Bay, California. Estuarine Coast Shelf Sci 73:538–550.

Smith L, Cheng RT. 1987. Tidal and tidally averaged circulation characteristics of Suisun Bay, California. Water Resources Res 23(1):143–155. doi: *http://dx.doi.org/10.1029/WR023i001p00143*

Stacey MT, Monismith SG, Burau JR. 1999. Observations of turbulence in a partially stratified estuary. J Phys Oceanogr 29:1950–1970. doi: *http://dx.doi.org/10.1175/1520-0485(1999)029<1950:OOTIAP>2.0.CO;2*

Stacey MT, Burau JR, Monismith SG. 2001. Creation of residual flows in a partially stratified estuary. J Geophys Res (Oceans) 106(C4):17013–17038. doi: *http://dx.doi.org/10.1029/2000JC000576*

Stacey MT, Ralston DK. 2005. The scaling and structure of the estuarine bottom boundary layer. J Phys Oceanogr 35:55–71. doi: *http://dx.doi.org/10.1175/JPO-2672.1*

Uncles RJ. 1982. Computed and observed residual currents in the Bristol Channel. Oceanologica Acta 5(1):11–20. Avalable from: *http://archimer.ifremer.fr/doc/00120/23148/*

Walters RA. 1982. Low-frequency variations in sea level and currents in South San Francisco Bay. J Phys Oceanogr 12:658–668. doi: *http://dx.doi.org/10.1175/1520-0485(1982)012<0658:LFVISL>2.0.CO;2*

Walters RA, Gartner JW. 1985. Subtidal sea level and current variations in the northern reach of San Francisco Bay. Estuarine Coast Shelf Sci 21:17–32. doi: *http://dx.doi.org/10.1016/0272-7714(85)90003-4*

http://dx.doi.org/10.15447/sfews.2016v14iss3art3

NOTES

These detailed measurements are an excerpt from a manuscript in preparation authored by MT Stacey, SG Monismith, LM Herdman, and R Holleman R, and titled, "Salt Dispersion in a Braided Channel Estuary." The data described below is available upon request to the corresponding author of this paper.

Suisun Bay Measurements Nov 2011–Jan 2012

As part of a larger study of the functioning of Suisun Bay sponsored by the United States Bureau of Reclamation, groups from U.C. Berkeley (Prof. Mark Stacey) and from Stanford (the author) deployed 11 moorings in the channels of Suisun Bay and the Western Delta for two months beginning in mid-November 2011. The data used in the present paper was taken at our station located near Chipps Island, where we deployed an upwards-looking 1200 KHz Teledyne RDI ADCP and two Seabird SBE-37 CTDs, one near-surface and one near-bottom. The ADCP data was recorded as single ping data and processed as described in Stacey et al (1999).